Diffusiophoresis of a Soft Spherical Particle in a Spherical Cavity

ARTICLE *in* THE JOURNAL OF PHYSICAL CHEMISTRY B · JULY 2009

Impact Factor: 3.3 · DOI: 10.1021/jp9014417 · Source: PubMed

4 AUTHORS, INCLUDING:

Wei-Lun Hsu
The University of Tokyo
17 PUBLICATIONS **128** CITATIONS

SEE PROFILE

Diffusiophoresis of a Soft Spherical Particle in a Spherical Cavity

Xiaogang Zhang

Department of Chemistry, Renmin University of China, Beijing, 100872, China

Wei-Lun Hsu and Jyh-Ping Hsu*

Department of Chemical Engineering, National Taiwan University, Taipei, Taiwan 10617

Shiojenn Tseng

Department of Mathematics, Tamkang University, Tamsui, Taipei, Taiwan 25137

Received: February 17, 2009; Revised Manuscript Received: May 6, 2009

The boundary effect on the diffusiophoresis of a colloidal particle is investigated theoretically by considering a soft spherical particle at an arbitrary position in a spherical cavity. The particle, which comprises a rigid core and an ion-penetrable layer, simulates biocolloids and particles covered by an artificial membrane layer. The diffusiophoretic behavior of the particle is governed by two types of DLP, the electrophoresis arising from the difference in the diffusivities of ionic species and diffusioosmotic flow. The influences of the thickness of the double layer, the size of the cavity, and the nature and the position of the particle on its diffusiophoretic behavior are discussed. We show that the presence of a boundary can have a profound influence on the behavior of a particle. The effect of electrophoresis can also lead to interesting diffusiophoretic behavior.

1. Introduction

Diffusiophoresis, the movement of colloidal particles driven by an applied concentration gradient, has many applications in practice. These include, for example, deposition of aerosols,[1−3] formation of surface coatings,[4,5] separation of particles,[6] and scavenging of radioactive particles,[7] to name a few. For nonelectrolyte solutions, the direction of particle migration depends upon the nature of solute−particle interaction.[8,9] The situation for electrolyte solutions becomes much more complicated.[10−14] In this case, three types of phenomena are involved if the particle is charged, namely, chemiphoresis,[15,16] electrophoresis,[17] and diffusioosmosis.[18] Chemiphoresis is due to the nonuniform accumulation of counterions and depletion of co-ions in the electrical double layer surrounding the particle, usually called double-layer polarization (DLP). Two kinds of DLP are identified: Type I DLP arises from the fact that the amount of counterions inside the double layer on the high concentration side of the particle is greater than that on the low concentration side. Type II DLP is due to the accumulation of co-ions coming from the applied concentration gradient near the outer boundary of the double layer on the high concentration side of the particle.[19] This phenomenon is important when the surface potential of the particle is sufficiently high. Electrophoresis comes from the electric field established by the electrolyte concentration gradient arising from the difference in ionic diffusivities. Diffusioosmosis includes electroosmosis and chemiosmosis. The former comes from the induced electric field arising from double-layer polarization, and the latter from the nonuniform ionic distribution in the double layer surrounding a particle.

* Corresponding author. Phone: 886-2-23637448. Fax: 886-2-23623040. E-mail: jphsu@ntu.edu.tw.

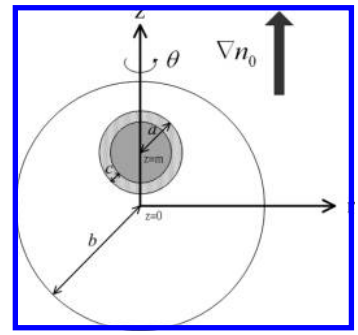

Figure 1. Diffusiophoresis of a soft spherical particle of radius a comprising a rigid core and an ion-penetrable layer of thickness c at an arbitrary position in a spherical cavity of radius b; r, θ, and z are the cylindrical coordinates adopted with the origin at the center of the cavity, and the applied concentration gradient ∇n_0 is in the z-direction.

Derjaguin et al.[20,21] initiated the study on diffusiophoresis and suggested that it was the mechanism of a process for depositing rubber latex films on a salt coated surface by considering a particle in an electrolyte solution. Considering both ionic and nonionic solutions, Staffeld and Quinn[22,23] performed both theoretical and experimental analyses on diffusiophoresis. The diffusiophoresis of polystyrene latex particles in an electrolyte solution was studied by Ebel et al.[24] Several attempts have been made on the investigation of the boundary effect on diffusiophoresis,[25−27] and the behavior of diffusioosmotic flow.[28−30] The interaction between a boundary and the double layer surrounding a particle was found to have a significant influence on the diffusiophoretic behavior of the particle. The presence of diffusioosmotic flow also plays an important role in diffusiophoresis.

Previous analyses on diffusiophoresis focused mainly on rigid particles.[11,13,17,19] Recently, the soft (or fuzzy) particle

10.1021/jp9014417 CCC: $40.75
Published on Web 06/01/2009

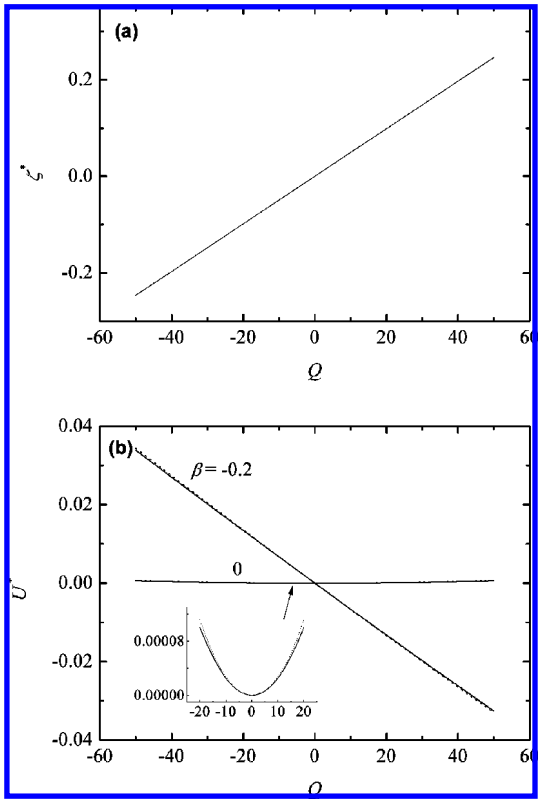

Figure 2. Variations of the scaled surface potential ζ^* (a) and the scaled diffusiophoretic velocity U^* (b) as a function of Q at various values of β. Solid curves, present results at $\alpha = 1$, $c/a = 0.01$, $\kappa a = 1$, $\Lambda = 0.05$, and $P = 0\%$; dotted curves, analytical results.[51]

model has been adopted by many researchers to simulate the electrophoretic behavior of biological cells and microorganisms,[31−36] subject to an applied electric field. A soft particle comprises a rigid core and an ion-penetrable layer[37] is capable of mimicking biocolloids and particles covered by an artificial membrane layer. It was shown that the presence of the ion-penetrable layer can influence appreciably the electrophoretic behavior of a particle. Note that, if the rigid core of a soft particle vanishes, it becomes an entirely porous one, and if its ion-penetrable layer vanishes, it reduces to the conventional rigid particle.

In this study, the boundary effect on the diffusiophoresis conducted in ionic solutions is investigated theoretically by considering a soft spherical particle in a spherical cavity taking account of the effects of electrophoresis and diffusioosmosis. The geometry considered is capable of modeling the behavior of a particle in a porous medium or in a cylindrical pore.[38] The ion-penetrable layer plays the role of, for example, the cell wall and fibrillar layer of biological cells. The thickness of this layer is ca. 10% or smaller of the linear size of nonfibrillated organisms, and can be larger than 30% of that of fibrillated organisms.[31,39] Many biological molecules such as proteins and DNA are polyelectrolytes, and can also be viewed as porous particles.[40] The influences of the key parameters, including the thickness of the double layer, the size of the cavity, and the nature and he position of the particle on its diffusiophoretic behavior are examined in detail.

2. Theory

The problem under consideration is illustrated in Figure 1, where a spherical particle of radius a is at an arbitrary position in a spherical cavity of radius b. Let $\Lambda = a/b$, which

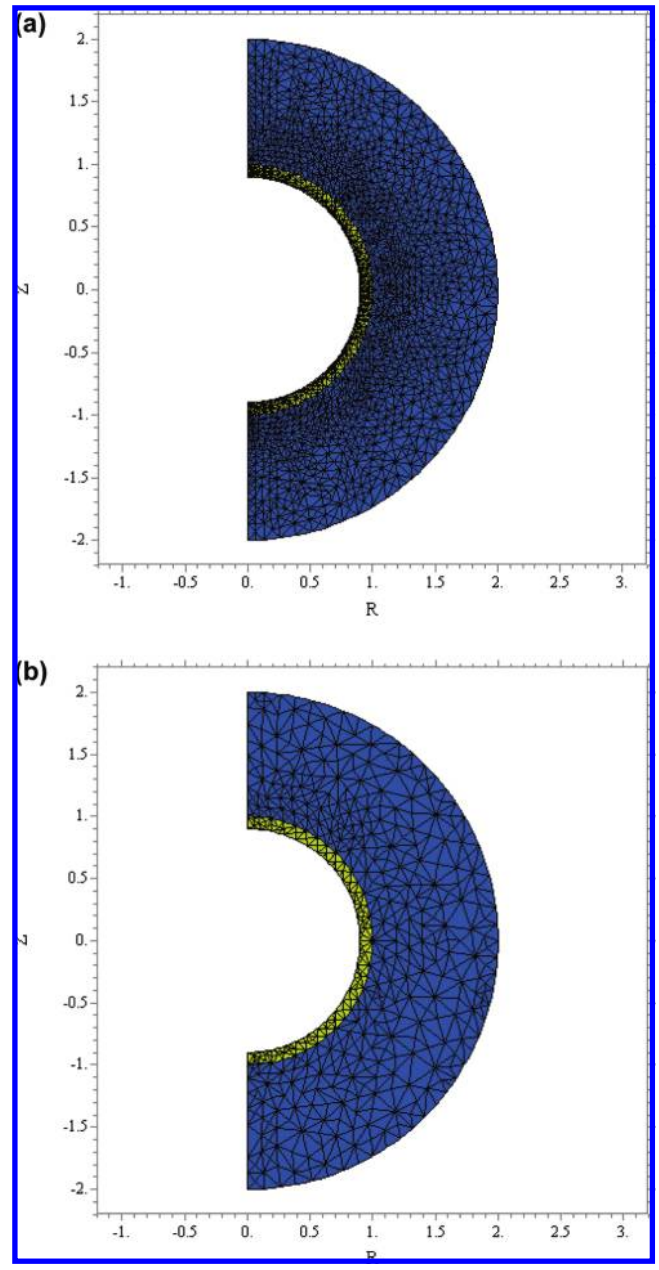

Figure 3. Example of the meshes used for the resolution of the electric field (a) and the flow field (b) on the half plane $\theta = 0$ at $\alpha = 1$, $\beta = 0$, $c/a = 0.1$, $\kappa a = 1$, $\Lambda = 0.5$, $P = 0\%$, and $Q = 50$.[50]

measures the significance of the boundary. The particle comprises a rigid core and an ion-penetrable membrane layer of thickness c, and the cavity is filled with an incompressible Newtonian fluid containing z_1:z_2 electrolytes, with z_1 and z_2 being the valences of cations and anions, respectively. r, θ, and z are the cylindrical coordinates adopted with the origin at the center of the cavity. The center of the particle is at $z = m$, and ∇n_0 is an applied uniform concentration gradient in the z-direction, with ∇ and n_0 being the gradient operator and the bulk concentration of the ionic species, respectively. For convenience, we assume that the particle is fixed and the cavity moves with the velocity $-U$, with U being the diffusiophoretic velocity of the particle.

If we let ϕ, $\mathbf{v}$, and n_j be the electrical potential, the velocity of the liquid phase, and the number concentration of ionic species j, respectively, then the phenomenon under consideration can be described by[12,41]

$$\nabla^2\phi = -\frac{\rho + i\rho_{\text{fix}}}{\varepsilon}, \quad i = 0, 1 \tag{1}$$

$$\nabla\cdot\left[-D_j\left(\nabla n_j + \frac{z_j e}{k_B T} n_j \nabla\phi\right) + n_j \mathbf{v}\right] = 0 \tag{2}$$

$$\nabla\cdot\mathbf{v} = 0 \tag{3}$$

$$-\nabla p + \eta\nabla^2\mathbf{v} - \rho\nabla\phi - i\gamma\mathbf{v} = 0, \quad i = 0, 1 \tag{4}$$

In these expressions, ∇^2 is the Laplace operator and i is a region index ($i = 1$ in an ion-penetrable layer, $i = 0$ outside the particle); ε, $\rho = \sum_{j=1}^{2} z_j e n_j$, and ρ_{fix} are the permittivity of the liquid phase, the space charge density of mobile ions, and the fix charge density in the ion-penetrable layer, respectively. D_j, z_j, e, k_B, and T are the diffusivity and the valence of ionic species j, the elementary charge, the Boltzmann constant, and the absolute temperature, respectively. η, p, and γ are the viscosity of the liquid phase, the pressure, and the frictional coefficient of the ion-penetrable layer, respectively. Equation 2 implies that the movement of ion species is influenced not only by the concentration gradient and the electric field but also by the liquid velocity, implying that there is relative velocity between ion species and the liquid. For simplicity, we assume that the distribution of the fixed charge is uniform, that is, ρ_{fix} is position independent.

For a simpler mathematical treatment, all of the dependent variables are partitioned into an equilibrium component, the value in the absence of ∇n_0, and a perturbed component, which arises from the application of ∇n_0: $\phi = \phi_e + \delta\phi$, $\mathbf{v} = \mathbf{v}_e + \delta\mathbf{v}$, $p = p_e + \delta p$, $n_j = n_{je} + \delta n_j$. Here, symbols with subscript e and prefix δ denote the equilibrium and the perturbed compo-

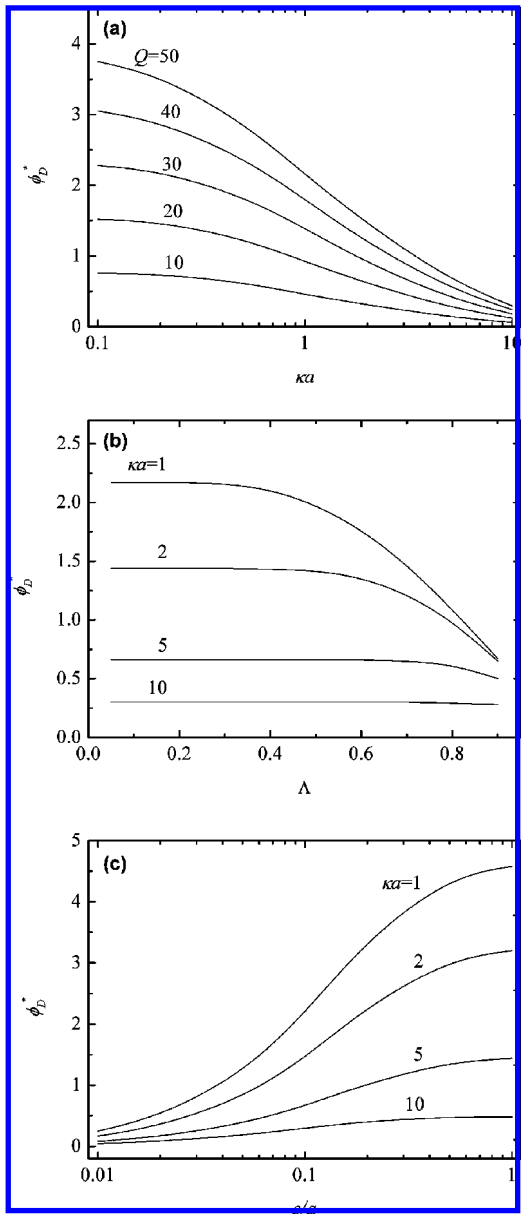

Figure 4. Variations of the scaled Donnan potential ϕ_D^* as a function of κa at various values of Q (a), as a function of Λ at various values of κa (b), and as a function of c/a at various values of κa (c). $\alpha = 1$, $c/a = 0.1$, $\Lambda = 0.2$, and $P = 0\%$ in part a, $c/a = 0.1$, $P = 0\%$, and $|Q| = 50$ in part b, and $\Lambda = 0.2$, $P = 0\%$, and $|Q| = 50$ in part c.

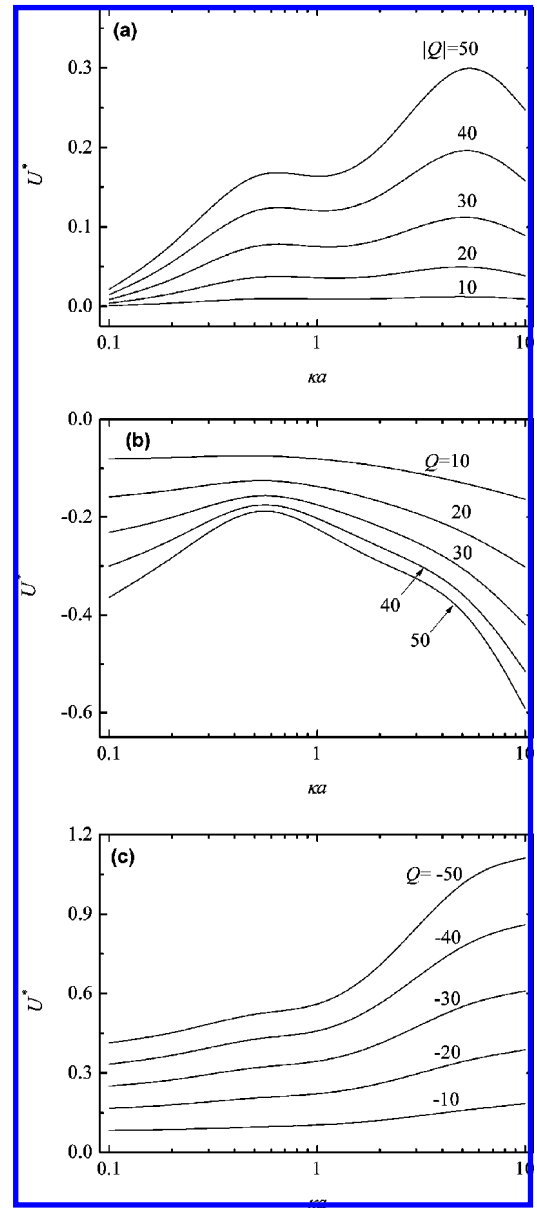

Figure 5. Variations of the scaled diffusiophoretic velocity U^* as a function of κa at various combinations of Q and β at $\alpha = 1$, $c/a = 0.1$, $\Lambda = 0.2$, and $P = 0\%$: (a) $\beta = 0$; (b) $\beta = -0.2$; (c) $\beta = -0.2$, $Q < 0$.

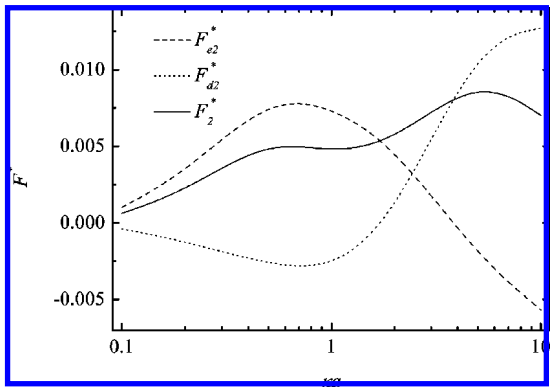

Figure 6. Variations of the scaled forces F^*_{e2}, F^*_{d2}, and F^*_2 as a function of κa for the case $|Q| = 50$ in Figure 5a.

nents, respectively. Note that $\mathbf{v}_e = \mathbf{0}$. A Boltzmann-type distribution is assumed for the spatial distribution of each mobile ionic species[41]

$$n_j = n_{j0e} \exp\left[-\frac{z_j e(\phi_e + \delta\phi + g_j)}{k_B T}\right], \quad j = 1, 2 \tag{5}$$

where n_{j0e} is the bulk ionic concentration at equilibrium. The presence of the perturbed function g_j, which simulates the deformation of the double layer surrounding the particle due to the convection term in eq 2, implies that the distribution of n_j is not exactly Boltzmann.

We assume that the distribution of ionic species is only slightly distorted over a length scale a after the application of ∇n_0, that is, $a|\nabla n_0| \ll n_{0e}$, where n_{0e} is the bulk solute concentration at equilibrium. In this case, because $\phi_e \gg \delta\phi + g_j$, expanding eq 5 into Taylor series and neglecting higher-order terms, we obtain

$$n_j = n_{j0e} \exp\left(-\frac{z_j e\phi_e}{k_B T}\right)\left[1 - \frac{z_j e}{k_B T}(\delta\phi + g_j)\right], \quad j = 1, 2 \tag{6}$$

On the basis of this expression, it can be shown that eqs 1 and 2 yield the following scaled equations:

$$\nabla^{*2}\phi^*_e = -\frac{(\kappa a)^2}{1+\alpha}[\exp(-\phi^*_e) - \exp(\alpha\phi^*_e)] - iQ \tag{7}$$

$$\nabla^{*2}\delta\phi^* = \frac{(\kappa a)^2}{1+\alpha}[(\delta\phi^* + g^*_1)\exp(-\phi^*_e) + \alpha(\delta\phi^* + g^*_2)\exp(\alpha\phi^*_e)] \tag{8}$$

$$\nabla^{*2}g^*_1 - \nabla^*\phi^*_e\cdot\nabla^* g^*_1 = \xi Pe_1 \mathbf{v}^*\cdot\nabla^*\phi^*_e \tag{9}$$

$$\nabla^{*2}g^*_2 + \alpha\nabla^*\phi^*_e\cdot\nabla^* g^*_2 = \xi Pe_2 \mathbf{v}^*\cdot\nabla^*\phi^*_e \tag{10}$$

where $\phi^*_e = \phi_e/(k_B T/z_1 e)$, $\delta\phi^* = \delta\phi/(k_B T/z_1 e)$, $\alpha = -z_2/z_1$, $\nabla^* = a\nabla$, $\nabla^{*2} = a^2\nabla^2$, and $g^*_j = g_j/(k_B T/z_1 e)$ are the scaled equilibrium potential, the scaled perturbed potential, the scaled gradient operator, the scaled Laplace operator, and the scaled form of g_j, respectively. $Q = \rho_{fix} a^2/\varepsilon(k_B T/z_1 e)$ denotes the scaled fixed charge density in the ion-penetrable layer; $\kappa = [\sum_{j=1}^{2} n_{j0e}(ez_j)^2/\varepsilon k_B T]^{1/2}$ is the reciprocal Debye length; $n^*_j = n_j/n_{j0e}$ and $Pe_j = \varepsilon(k_B T/z_1 e)^2/\eta D_j$ are the scaled number density and the electric Peclet number of ionic species j, respectively. $\mathbf{v}^* = \mathbf{v}/U^0$ is the scaled liquid velocity, where $U^0 = \varepsilon\xi\,(k_B T/z_1 e)^2/a\eta$ is a reference velocity; $\xi = \nabla^* n^*_0$ is the scaled concentration gradient imposed to the system, and $n^*_0 = n_0/n_{0e}$.

In terms of the scaled symbols, it can be shown that eqs 3 and 4 become[42−44]

$$\nabla^*\cdot\mathbf{v}^* = 0 \tag{11}$$

$$-\nabla^*\delta p^* + \xi\nabla^{*2}\mathbf{v}^* + (\nabla^{*2}\phi^*_e + iQ\nabla^*\delta\phi^* + \nabla^{*2}\delta\phi^*\nabla^*\phi^*_e) - i\xi(\lambda a)^2\mathbf{v}^* = 0 \tag{12}$$

where $\delta p^* = \delta p/[\varepsilon(k_B T/z_1 e)^2/a^2]$ and $\lambda = (\gamma/\eta)^{1/2}$. Intuitively, ρ_{fix} correlates positively with γ. For convenience, we assume that $\rho_{fix} \propto \gamma$ and $Q = (\lambda a)^2$, which yield $\rho_{fix} = \varepsilon(k_B T/z_1 e)\gamma/\eta$.

We assume that the surface of the rigid core of the particle is uncharged, nonconductive, impermeable to ionic species,[45] and nonslip. These yield the following boundary conditions:

$$\mathbf{n}\cdot\nabla\phi^*_e = 0 \tag{13}$$

$$\mathbf{n}\cdot\nabla^*\delta\phi^* = 0 \tag{14}$$

$$\mathbf{n}\cdot\nabla^* g^*_j = 0 \tag{15}$$

$$\mathbf{v}^* = 0 \tag{16}$$

We consider the case where the cavity surface is uncharged and nonslip. The concentration of ionic species is assumed to reach the corresponding bulk level on the cavity surface. The electric current arising from the diffusion and the electric migration of ions is negligible, and the net charge flux due to the diffusioosmotic flow vanishes in the bulk liquid phase. These assumptions lead to the following boundary conditions on the cavity surface:

$$\phi^*_e = 0 \tag{17}$$

$$\mathbf{n}\cdot\nabla^*\delta\phi^* = \Lambda\beta\xi z^* \tag{18}$$

$$g^*_1 = -(z^* - m^*)\xi - \delta\phi^* \tag{19}$$

$$g^*_2 = \frac{(z^* - m^*)\xi}{\alpha} - \delta\phi^* \tag{20}$$

$$\mathbf{v}^* = -U^*\mathbf{e}_z \tag{21}$$

where $\beta = [D_1 - D_2]/[D_1 + \alpha D_2]$, $U^* = U/U^0$, $z^* = z/a$, $\mathbf{n}$ is the unit normal vector directed into the liquid phase, and $\mathbf{e}_z$ is

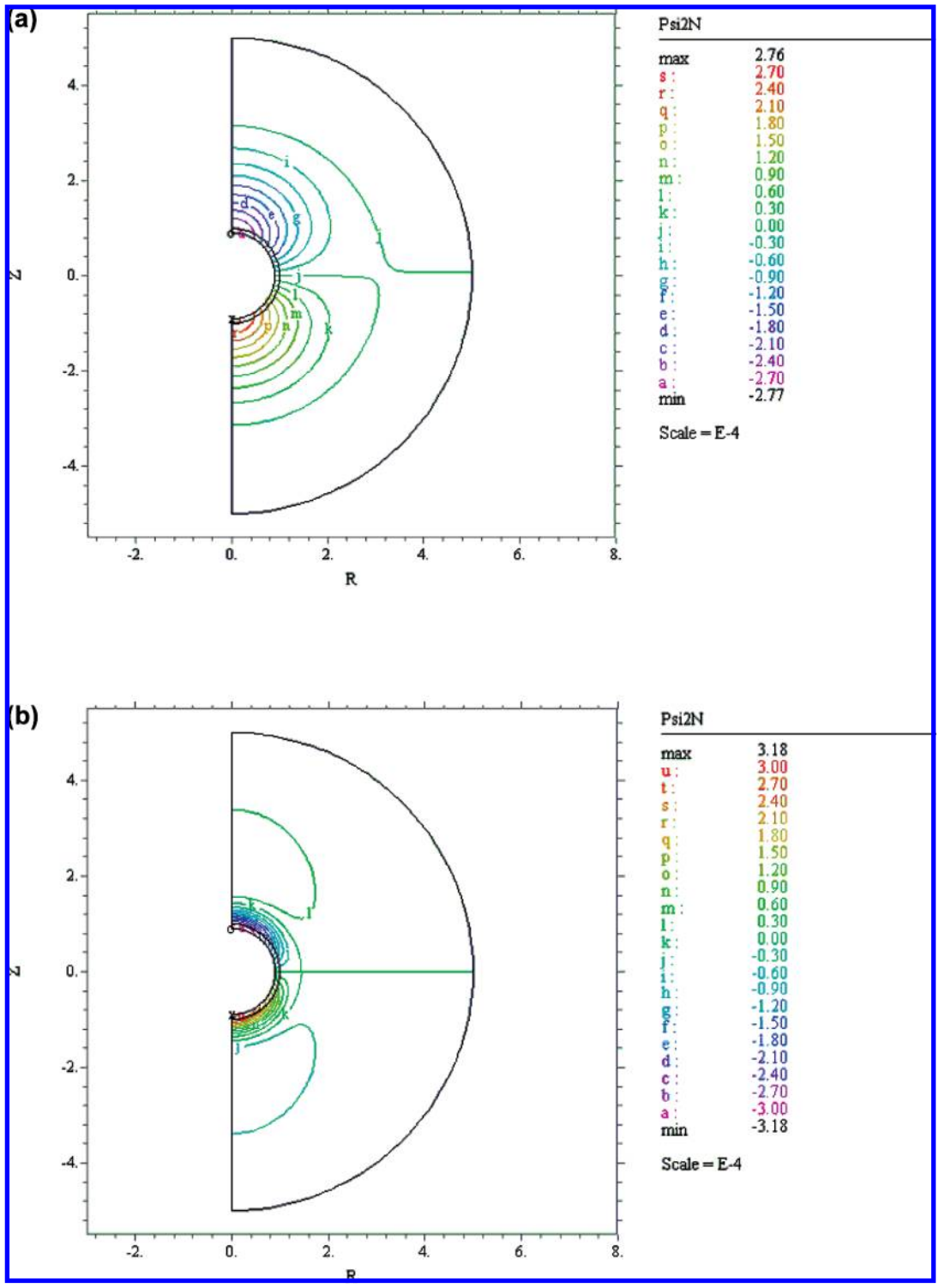

Figure 7. Contours of the scaled disturbed electric potential $\delta\phi^*$ on the half plane $\theta = 0$, phi2N, for different levels of κa at $\alpha = 1$, $\beta = 0$, $c/a = 0.1$, $\Lambda = 0.2$, $P = 0\%$, and $Q = 50$: (a) $\kappa a = 1$; (b) $\kappa a = 5$.

the unit vector in the z-direction. Note that eqs 19 and 20 imply that the ionic concentration on the cavity surface is $n_{j0e} + (z - m)\nabla n_{j0}$.[46]

Note that, on the membrane−liquid interface ϕ_e^*, $\mathbf{n}\cdot\nabla\phi_e^*$, $\mathbf{v}^*$, $\mathbf{n}\cdot\mathbf{v}^*$, $\mathbf{n} \times \mathbf{v}^*$, $\mathbf{n}\cdot(\mathbf{n}\cdot\boldsymbol{\sigma}^{\mathbf{H}^*})$, and $\mathbf{n} \times (\mathbf{n}\cdot\boldsymbol{\sigma}^{\mathbf{H}^*})$ should be continuous, where $\boldsymbol{\sigma}^{\mathbf{H}^*} = \boldsymbol{\sigma}^{\mathbf{H}}/[\varepsilon(k_BT/z_1e)^2a^2]$ is the scaled form of the shear stress tensor $\boldsymbol{\sigma}^{\mathbf{H}} = -\delta p\mathbf{I} + 2\eta\boldsymbol{\Delta}$; $\mathbf{I}$ is the unit tensor; $\boldsymbol{\Delta} = [\nabla\delta\mathbf{v} + (\nabla\delta\mathbf{v})^T]/2$ is the rate of deformation tensor; the superscript T represents matrix transpose. However, due to the nature of that interface, specifying the continuous boundary condition is unnecessary because it is satisfied automatically in the solution produce.

Following the similar treatment of O'Brien and White,[41] where the motion of a particle is driven by an applied electric field, we partition the present problem into two hypothetical subproblems. In the first subproblem, the cavity moves at a constant velocity $-U$ when ∇n_0 is not applied, and in the second subproblem, ∇n_0 is applied but the cavity is held fixed.

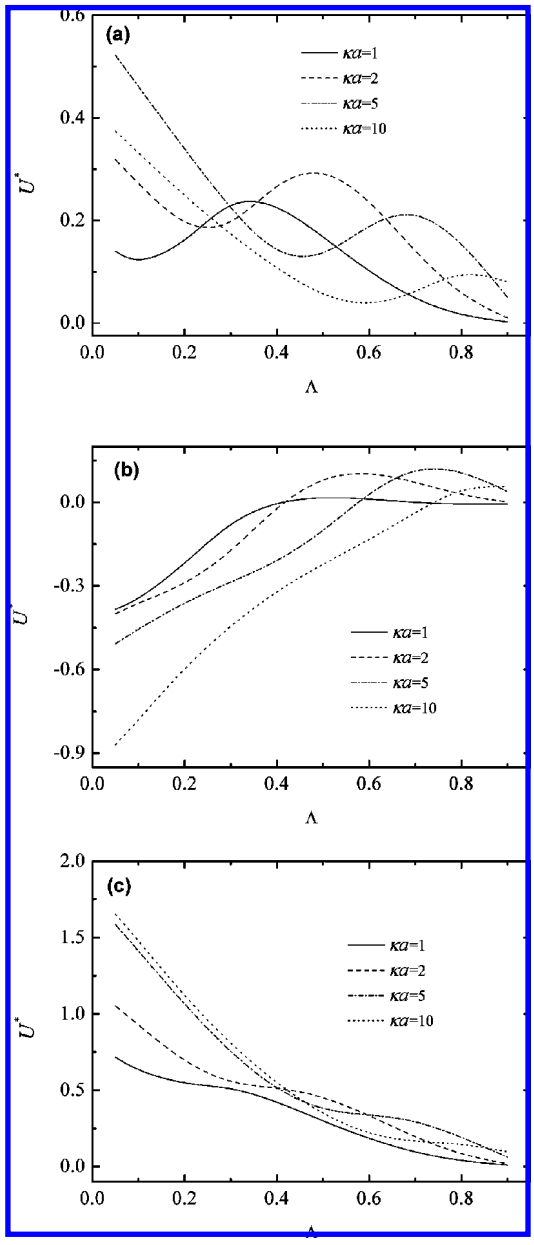

Figure 8. Variations of the scaled diffusiophoretic velocity U^* as a function of Λ at various combinations of κa and β at $\alpha = 1$, $c/a = 0.1$, and $P = 0\%$: (a) $\beta = 0$, $|Q| = 50$; (b) $\beta = -0.2$, $Q = 50$; (c) $\beta = -0.2$, $Q = -50$.

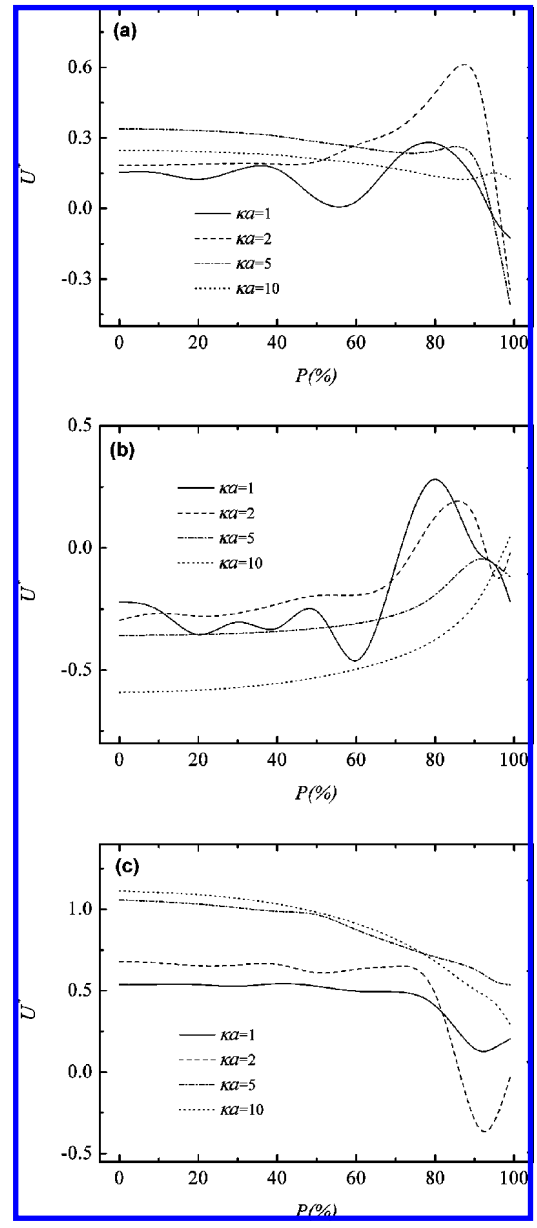

Figure 10. Variations of the scaled diffusiophoretic velocity U^* as a function of the position parameter P for various combinations of κa, β, and Q at $\alpha = 1$, $c/a = 0.1$, and $\Lambda = 0.2$: (a) $\beta = 0$, $|Q| = 50$; (b) $\beta = -0.2$, $Q = 50$; (c) $\beta = -0.2$, $Q = -50$.

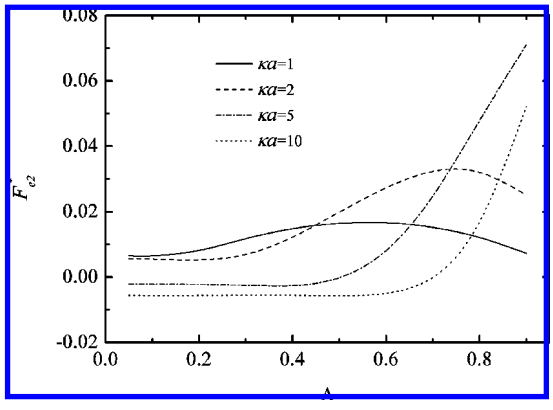

Figure 9. Variations of the scaled electrical force F^*_{e2} as a function of Λ for the case of Figure 8a.

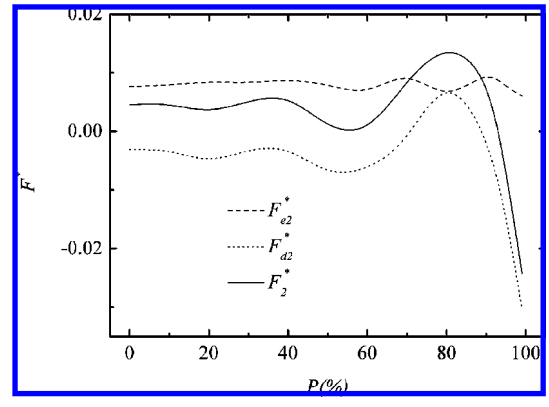

Figure 11. Variations of the scaled forces F^*_{e2}, F^*_{d2}, and F^*_2 as a function of P for the case $\kappa a = 1$ and $|Q| = 50$ in Figure 10a.

In the first subproblem, the force acting on the particle in the z-direction can be expressed as $F_1 = F_{e1} + F_{d1} = \chi_1 U$, where χ_1 is independent of U, and F_{e1} and F_{d1} are the z-components of the electric force and the hydrodynamic force, respectively. In the second subproblem, the force acting on the particle in the z-direction can be expressed as $F_2 = F_{e2} + F_{d2} = \chi_2 \nabla n_0$, where F_{e2} and F_{d2} are the z-components of the electric force and the hydrodynamic force, respectively, and the latter arises from the movement of the ionic species in the double layer. Note that χ_2 is independent of ∇n_0. Because the total force acting on the particle in the z-direction vanishes under steady-state conditions, $F_1 + F_2 = 0$, which yields $U = -(\chi_2/\chi_1)\nabla n_0$. If we let $F^*_{ej} = F_{ej}/\varepsilon(k_B T/z_1 e)^2$ and $F^*_{dj} = F_{dj}/\varepsilon(k_B T/z_1 e)^2$, $j = 1, 2$, it can be shown that[46−48]

$$F^*_{ej} = \int_{S^*} (\boldsymbol{\sigma}^{E^*} \cdot \mathbf{n}) \cdot \mathbf{e}_z \, dS^* = \int_{S^*} \left[\left(\frac{\partial \phi_1^*}{\partial n} \frac{\partial \phi_2^*}{\partial z^*} + \frac{\partial \phi_2^*}{\partial n} \frac{\partial \phi_1^*}{\partial z^*} \right) - \left(\frac{\partial \phi_1^*}{\partial n} \frac{\partial \phi_2^*}{\partial n} + \frac{\partial \phi_1^*}{\partial t} \frac{\partial \phi_2^*}{\partial t} \right) n_z \right] dS^*, \quad j = 1, 2 \tag{22}$$

$$F^*_{dj} = \int_{S^*} (\boldsymbol{\sigma}^{H^*} \cdot \mathbf{n}) \cdot \mathbf{e}_z \, dS^*, \quad j = 1, 2 \tag{23}$$

where $S^* = S/a^2$, with S being the particle surface, and n and t are the magnitude of the unit normal vector $\mathbf{n}$ and that of the unit tangential vector $\mathbf{t}$, respectively.

3. Results and Discussion

The nonlinear and coupled nature of the governing equations prevents us from solving them analytically. This difficulty is circumvented by adopting FlexPDE,[50] a commercial software based on the finite element method. The applicability of this software is justified by solving the diffusiophoresis of an isolated, rigid, positively charged sphere in an infinite aqueous solution where an analytical solution is available.[48] For comparison, we let $c/a \ll 1$ and $c/a \ll \kappa a^{-1}$ so that the present soft particle reduces to a rigid particle of constant surface charge. In this case, Q is proportional to the surface potential, ζ, as illustrated in Figure 2a, where $\zeta^* = \zeta/(k_B T/z_1 e)$ is plotted against Q. Furthermore, if Λ is sufficiently small, the present problem is close to an isolated sphere in an infinite fluid.[51] The results of Figure 2b are based on this condition. This figure reveals that the performance of the present numerical approach is satisfactory.

The influences of the key parameters on the diffusiophoretic behavior of a particle are investigated through numerical simulation. These include the thickness of the double layer, the nature of the particle and its position in the cavity, and the nature of ions in the liquid phase. Typically, using a total of 8337 and 1994 nodes is sufficient to achieve grid independence. An example of mesh structure is illustrated in Figure 3.

Donnan Potential ϕ_D. Referring to Figure 4, let us examine first the behavior of the scaled Donnan potential $\phi^*_D = \phi_D/(k_B T/z_1 e)$, where ϕ_D is the potential on the surface of the rigid core of a particle, under various conditions. In the present case, ϕ^*_D is positive. Figure 4a shows that ϕ^*_D decreases with increasing κa. This can be explained by the fact that, as κa increases, that is, the ionic concentration increases and the thickness of the double layer decreases, then the amount of counterions penetrated into the ion-penetrable layer of the particle increases, yielding a decrease in the net charge density, $|\rho + \rho_{fix}|$. As seen in Figure 4b, if κa is small (double layer is thick), then ϕ^*_D decreases with increasing Λ (=a/b), but it remains essentially constant if κa is large. This is because, if Λ is large, the boundary (cavity) effect is significant. In this case, the double layer is compressed, driving counterions into the ion-penetrable layer of the particle. This effect is enhanced if the double layer is thick. On the other hand, if the double layer is thin (large κa), then that boundary effect becomes unimportant. The behavior of ϕ^*_D in Figure 4c is expected because the larger the (c/a), the thicker the ion-penetrable layer, and therefore the larger the amount of charge inside.

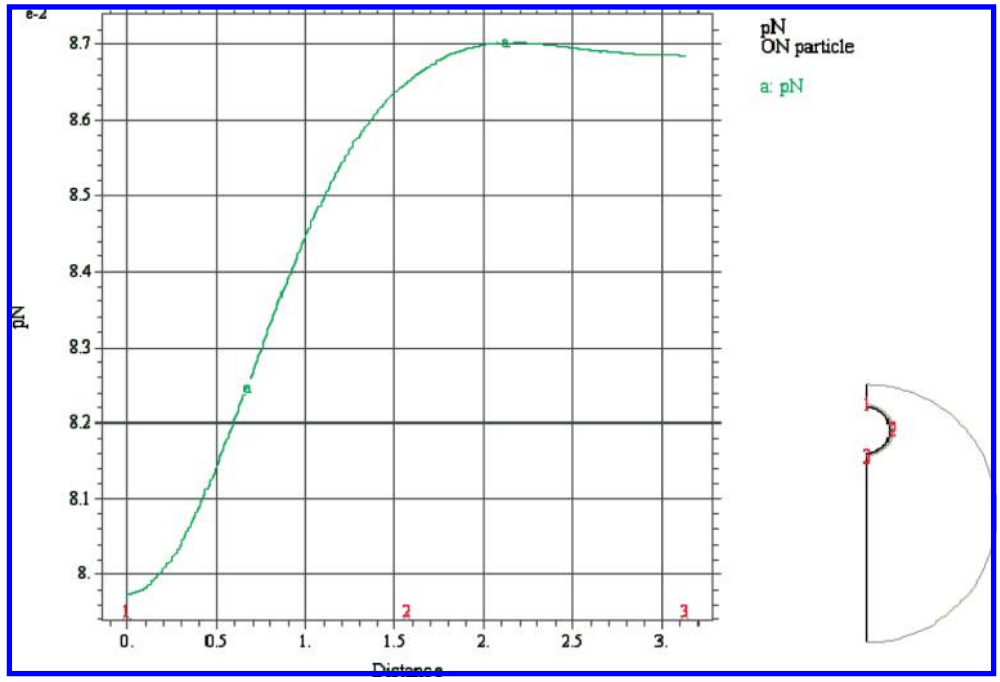

Figure 12. Spatial variation in the scaled disturbed pressure δp^* on the half plane $\theta = 0$, at $\alpha = 1$, $\beta = 0$, $c/a = 0.1$, $\kappa a = 1$, $\Lambda = 0.2$, $P = 80\%$, and $|Q| = 50$.

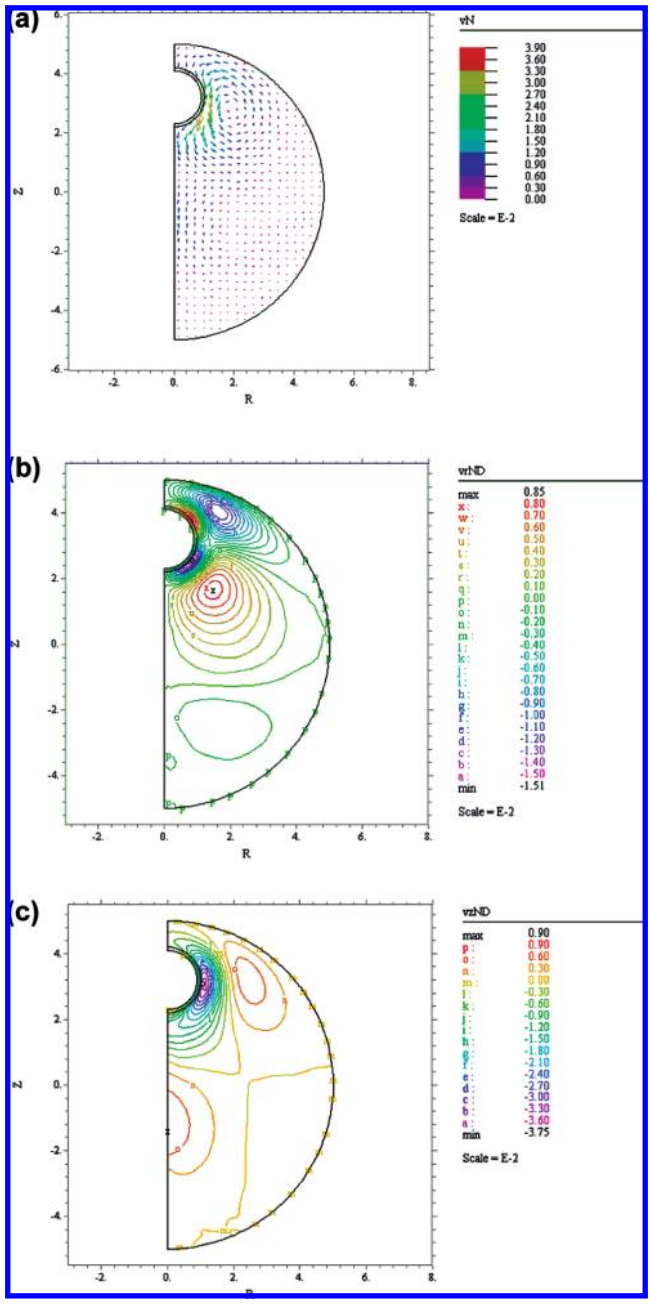

Figure 13. Contours of the scaled velocity **v*** on the half plane $\theta = 0$, vN (a), that of the scaled velocity in the r-direction, vrND (b), and that of the scaled velocity in the z-direction, vzND (c), at $\alpha = 1$, $\beta = 0$, $c/a = 0.1$, $\kappa a = 1$, $\Lambda = 0.2$, $P = 80\%$, and $|Q| = 50$.

Effect of Double Layer Thickness κa. Figure 5 presents the variations of the scaled diffusiophoretic velocity U^* as a function of κa at various combinations of Q and β. Note that $\beta = 0$ and $Pe_1 = Pe_2 = 0.26$, which corresponds to KCl solution, in Figure 3a, implying that the particle is driven solely by chemiphoresis. On the other hand, $\beta = -0.2$, $Pe_1 = 0.39$, and $Pe_2 = 0.26$, which corresponds to NaCl solution, in Figure 5b and c, implying that the particle is driven both by chemiphoresis and by electrophoresis. Figure 5a shows that U^* has two local maxima, one at $\kappa a \cong 0.5$ and the other at $\kappa a \cong 5.5$. As justified by Figure 6, this arises from the competition between types I and II DLP and the diffusioosmotic flow (chemiosmotic flow at $\beta = 0$). As seen in this figure, F^*_{e2} has a local maximum at $\kappa a \cong 0.7$, and $F^*_{e2} < 0$ for $\kappa a > 4$. These arise from the competition between types I and II DLP. If κa is small, F^*_{e2} is dominated by type I DLP, yielding an electric field which drives the particle toward the high concentration side. On the other

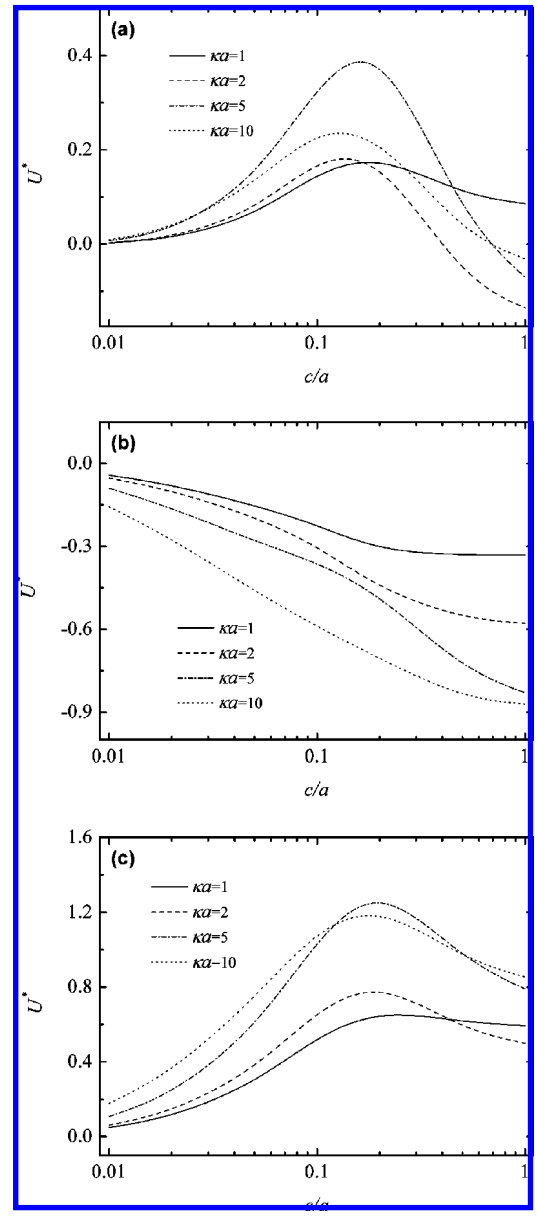

Figure 14. Variations of the scaled diffusiophoretic velocity U^* as a function of c/a at various combinations of κa, β, and Q at $\alpha = 1$, $\Lambda = 0.2$, and $P = 0\%$: (a) $\beta = 0$, $|Q| = 50$; (b) $\beta = -0.2$, $Q = 50$; (c) $\beta = -0.2$, $Q = -50$.

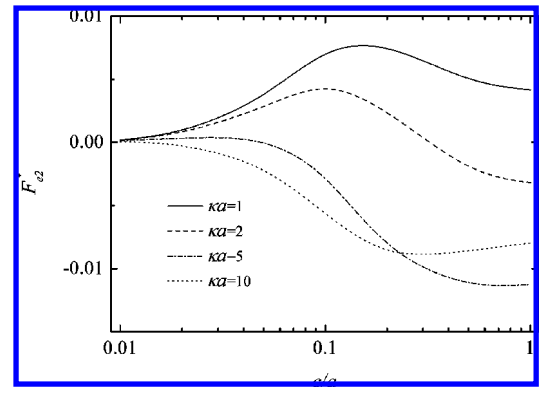

Figure 15. Variations of the scaled electrical force F^*_{e2} as a function of c/a for the case of Figure 14a.

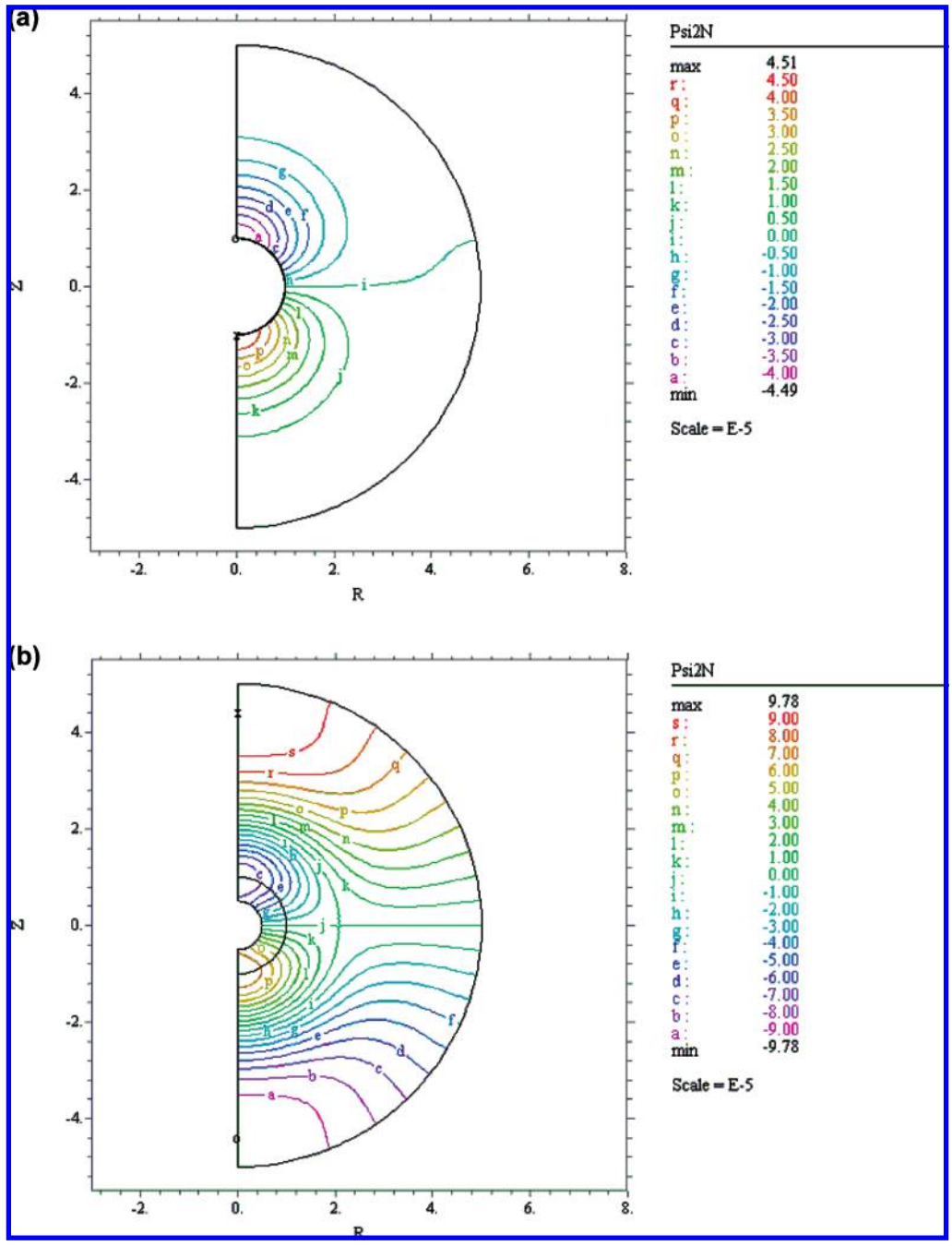

Figure 16. Contours of the scaled disturbed electric potential $\delta\phi^*$ on the half plane $\theta = 0$, phi2N, for two levels of c/a at $\alpha = 1$, $\beta = 0$, $\Lambda = 0.2$, $\kappa a = 1$, $P = 0\%$, and $Q = 50$: (a) $c/a = 0.01$; (b) $c/a = 0.5$.

hand, if κa is small, then type II DLP dominates which drives the particle toward the low concentration side. As κa increases, the amount of counterions penetrated into the ion-penetrable layer increases accordingly, which reduces the net amount of charge inside. Meanwhile, due to the stronger electric repulsive force between co-ions and the particle, more co-ions accumulated near the surface of the particle, enhancing type II DLP. Therefore, the scaled disturb potential $\delta\phi^*$ becomes positive in the outer region of the double layer, as shown in Figure 7b. Figure 6 also indicates that F_{32}^* is negative for small κa and positive for large κa. Because type I DLP induces an electric field, which drives counterions from the high concentration to the low concentration, if it dominates, chemiphoosmotic flow tends to flow along the same direction over the particle surface. On the other hand, the electric field induced by type II DLP is in the opposite direction, and therefore, if it dominates, the direction of the accompanying chemiphoosmotic flow is opposite too. In Figure 5b and c, because $\beta \neq 0$, the effect of electrophoresis needs to be taken into account. In these cases, if the particle is positively charged, U^* is smaller than that in Figure 5a, and is larger than that in Figure 5a if it is negatively charged. This is because, if $\beta < 0$, the difference between the diffusivity of cations and that of anions yields an electric field, which is in the opposite direction as that of ∇n_0, and the magnitude of this electric field is $|\beta\xi|$, as illustrated in eq 22. As can be inferred from Figure 5b, the larger the scaled fixed charge density Q, the more significant the effect of electrophoresis. Furthermore, although the value of U^* at $Q = 50$ is the largest in Figure 5a, it becomes the smallest in Figure 5b. This implies that the effect of electrophoresis is more important than that of chemiphoresis in this case. As will be explained later, the effects of electrophoresis and chemiphoresis are related

to Λ. Note that the difference in U^* between $\beta = 0$ and $\beta = -0.2$ increases with increasing κa. For instance, the difference in U^* between the cases in Figure 5a and b is ca. 0.39 at $\kappa a = 0.1$ and $Q = 50$ and is ca. 0.84 at $\kappa a = 10$ and $Q = 50$. This implies that the higher the concentration of electrolytes, the more important the effect of electrophoresis.

Effect of Cavity Size Λ. The variations of the scaled diffusiophoretic velocity U^* as a function of Λ ($=a/b$), which measures the significance of the boundary effect, under various conditions are presented in Figure 8. As seen in Figure 8a, for small Λ, U^* decreases roughly linearly with increasing Λ, and exhibits a local maximum at a large value of Λ. Note that, if Λ is sufficiently small, then the double layer does not touch the cavity, and therefore, although the size of the cavity decreases with increasing Λ, the double layer is not compressed by the cavity. Therefore, as seen in Figure 9, the scaled electric force F_{e2}^* arising from DLP remains essentially constant. The decrease in U^* comes mainly from the fact that the presence of the boundary increases the hydrodynamic drag acting on the particle. If Λ is sufficiently large, the cavity is entirely filled by the double layer. In this case, an increase in Λ results in more ions to be driven into the ion-penetrable layer and also to the surface of the particle by the cavity. The former yields a lower charge density in the ion-penetrable layer and a lesser degree of types I and II DLP. The latter leads to a higher charge density near the particle surface, and enhances both types I and II DLP. Figure 9 suggests that, if κa is sufficiently large, F_{e2}^* increases with increasing Λ. This is because, if the ion-penetrable layer is thin and $Q = (\lambda a)^2$ is large ($=50$), only a small amount of ions can penetrate into the ion-penetrable layer. Therefore, the effect due to the drive of ions by the cavity to the particle surface is more important than that due to the drive of ions driven by the cavity into the ion-penetrable layer. For both $\kappa a = 1$ and $\kappa a = 2$, F_{e2}^* has a local maximum as Λ varies, which arises from the competition between types I and II DLP. In addition, F_{e2}^* increases when the double layer is compressed, implying that the increase in the degree of type I DLP is larger than that of type II DLP. Compared with that in Figure 8a, U^* in Figure 8b and c varies appreciably when Λ is small but remains roughly constant at large Λ. This implies that the effect of electrophoresis at small Λ is more important than that at large Λ.

Effect of Particle Position *P*. The influence of the position of a particle, measured by the position parameter $P = 100\% \times [m/(b - a)]$, on its scaled diffusiophoretic velocity is illustrated in Figure 10. Figure 10a shows that U^* has a local maximum at a large value of P. It is interesting to see that, if the double layer is thick ($\kappa a = 1$), the U^* against P curve oscillates. However, as κa gets large, that oscillation becomes inappreciable. If κa is large, the double layer is thin relative to the cavity radius, and therefore, the double layer is not compressed by the cavity even if P is large. In this case, the increase in P only raises the hydrodynamic drag acting on the particle, but the electric force F_{e2}^*, which may arise from types I and II DPL, remains roughly constant. That is, the decrease of U^* with increasing P for large values of P seen in Figure 10a arises mainly from the increase of the hydrodynamic drag. However, if κa is small ($=1$), the compression of the double layer by the cavity is important even if the particle is at the center of the cavity ($P = 0\%$). In this case, if the particle is closer to the top of the cavity, the degree of double-layer compression is more serious on the high concentration side than that on the low concentration side. Therefore, both types I and II DLP increase on the high concentration side and decrease on the low concentration side. In addition, if $P \neq 0$, the system is not r-symmetric, making the behavior of the particle even more complicated. As seen in Figure 10a, for both large κa and small κa, U^* shows a local maximum at a large P (>75%). As illustrated in Figure 11, the presence of the local maximum arises mainly from F_{d2}^* because, if the particle is close to the cavity, the chemiosmotic flow arising from type I DLP drives the particle upward. Note that, although the chemiosmotic flow near the particle surface is still from the high concentration side to the low concentration side, the pressure becomes very small at the top of the particle. This is because, if the particle is close to the cavity, the space between the two is small, and the fluid flow out from that space yields a pressure reduction. As seen in Figure 12, the scaled disturb pressure δp^* has the smallest value at the top of the particle. The conservation of mass implies that the fluid must flow back to the space between the top of the particle and the cavity along the cavity surface, as seen in Figure 13. This flow drives the particle toward the low concentration side (i.e., downward). The competition of the above-mentioned two flows yields a local maximum in U^* at a large P. Note that, except for $\kappa a = 1$, U^* has the minimum value at $P = 0\%$ in Figure 8b and the maximum value at $P = 0\%$ in Figure 10c. These imply that the effect of electrophoresis is more important at small P. The behavior of U^* at large P becomes complicated because, if $\beta \neq 0$, the diffusioosmotic flow is contributed by both chemiosmotic flow and electroosmotic flow. For a positively charged particle at $\beta = -0.2$, the direction of the electroosmotic flow is opposite to that of the chemiosmotic flow. Therefore, the diffusioosmotic flow is reduced, and even can change its direction from the low concentration side to the high concentration side. For a negatively charged particle at $\beta = -0.2$, the direction of the electroosmotic flow is the same as that of the chemiosmotic flow, and the diffusioosmotic flow is enhanced.

Effect of Ion-Penetrable Layer Thickness (c/a). The influence of the thickness of the ion-penetrable layer of a particle on its scaled diffusiophoretic velocity under various conditions is illustrated in Figure 14. The presence of the local maximum of U^* in Figure 14a is due to the competition between types I and II DLP. Referring to Figure 15, if κa is small, F_{e2}^* is dominated by type I DLP at small c/a. In this case, because the amount of fixed charge in the ion-penetrable layer increases with increasing c/a, U^* increases accordingly. However, as seen in Figure 16, if c/a is large, the amount of counterions penetrated is appreciable and the amount of co-ions accumulated near the surface of the particle becomes important, leading to a significant type II DLP. In this case, U^* decreases with increasing c/a. As seen in Figure 14a, U^* ($\kappa a = 10$) > 0 at small c/a even if F_{e2}^* (<0) is dominated by type II DLP. This implies that, at large κa, F_{d2}^* is more important than F_{e2}^* at small c/a. Figure 14b and c suggests that the effect of electrophoresis is more important when c/a is sufficiently large (>0.1). This is because the total amount of charge in the ion-penetrable layer of a particle increases with increasing c/a, and the electric force acting on the particle increases accordingly.

4. Conclusions

In summary, the boundary effect on diffusiophoreis is analyzed theoretically by considering a soft spherical particle in a spherical cavity. The soft particle, which comprises a rigid core and an ion-penetrable layer, is capable of simulating biocolloids and particles covered by an artificial membrane layer. We show that, in addition to the nature of the particle, its diffusiophoretic behavior is governed by two types of DLP and

the effect of electrophoresis. The influences of the key parameters of the system under consideration on the diffusiophoreis of a particle can be summarized as follows. If the particle is driven solely by chemiphoresis, the scaled diffusiophoretic mobility has two local maxima as the thickness of the double layer varies. Depending upon the charged conditions of a particle, the presence of the electrophoresis effect can reduce or raise its diffusiophoretic mobility. If the boundary effect is insignificant, the effect of electrophoresis is more important than the effect of chemiphoresis. In addition, the higher the ionic concentration, the more important the effect of electrophoresis. If the cavity is large, the scaled diffusiophoretic mobility decreases roughly linearly with decreasing cavity radius and passes through a local maximum at a cavity radius that is close to the particle size. The effect of electrophoresis is more important at the following conditions: larger cavity radius, the particle is closer to the cavity center, and the thicker the ion-penetrable layer. The variation in the position of the particle can lead to complicated diffusiophoretic behavior, especially when the double layer is thick.

Acknowledgment. This work is supported by the National Science Council of the Republic of China and the National Nature Science Foundation of China (20876169).

References and Notes

(1) Hidy, G. M.; Brock, J. R. *Environ. Sci. Technol.* **1969**, *3*, 563.
(2) Munoz-Cobo, J. L.; Pena, J.; Herranz, L. E.; Perez-Navarro, A. *Nucl. Eng. Des.* **2005**, *235*, 1225.
(3) Dukhin, S. S.; Ulberg, Z. R.; Dvornichenko, G. L.; Deryagin, B. V. *Bull. Acad. Sci. USSR Div. Chem. Sci.* **1982**, *31*, 1535.
(4) Dvornichenko, G. L.; Nizhnik, Y. V.; Slavikovskii, T. V.; Nikolaichuk, L. V. *Colloid J. Rus. Acad. Sci.* **1993**, *55*, 36.
(5) Ulberg, Z. R.; Ivzhenko, N. N.; Dvornichenko, G. L.; Buadze, R. O.; Koniashvili, S. A. *Ukr. Khim. Zh.* **1992**, *58*, 390.
(6) Meisen, A.; Bobkowic, A. J.; Cooke, N. E.; Farkas, E. J. *Can. J. Chem. Eng.* **1971**, *49*, 449.
(7) Goldsmith, P.; Delafield, H. J.; Cox, L. C. *Q. J. R. Meteorol. Soc.* **1963**, *89*, 43.
(8) Anderson, J. L.; Lowell, M. E.; Prieve, D. C. *J. Fluid Mech.* **1982**, *117*, 107.
(9) Keh, H. J.; Wan, Y. W. *Chem. Eng. Sci.* **2008**, *63*, 1612.
(10) Prieve, D. C.; Anderson, J. L.; Ebel, J. P.; Lowell, M. E. *J. Fluid Mech.* **1984**, *148*, 247.
(11) Prieve, D. C.; Roman, R. *J. Chem. Soc., Faraday Trans. 2* **1987**, *83*, 1287.
(12) Wei, Y. K.; Keh, H. J. *J. Colloid Interface Sci.* **2002**, *248*, 76.
(13) Hsu, J. P.; Lou, J.; He, Y. Y.; Lee, E. *J. Phys. Chem. B* **2007**, *111*, 2533.
(14) Abecassis, B.; Cottin-Bizonne, C.; Ybert, C.; Ajdari, A.; Bocquet, L. *Nat. Mater.* **2008**, *7*, 785.
(15) Prieve, D. C.; Gerhart, H. L.; Smith, R. E. *I&EC Prod. R&D* **1978**, *17*, 32.
(16) Prieve, D. C.; Gerhart, H. L.; Sander, R. A.; Smith, R. E. *J. Colloid Interface Sci.* **1979**, *71*, 267.
(17) Pawar, Y.; Solomentsev, Y. E.; Anderson, J. L. *J. Colloid Interface Sci.* **1993**, *155*, 488.
(18) Keh, H. J.; Ma, H. C. *Langmiur* **2005**, *21*, 5461.
(19) Hsu, J. P.; Hsu, W. L.; Chen, Z. S. *Langmuir* **2009**, *25*, 1772.
(20) Deryagin, B. V.; Dukhin, S. S.; Korotkova, A. A. *Mikrobiologiya* **1961**, *13*, 53.
(21) Deryagin, B. V.; Dukhin, S. S.; Korotkova, A. A. *Kolloidn. Zh.* **1961**, *23*, 53.
(22) Staffeld, P. O.; Quinn, J. A. *J. Colloid Interface Sci.* **1988**, *130*, 69.
(23) Staffeld, P. O.; Quinn, J. A. *J. Colloid Interface Sci.* **1988**, *130*, 88.
(24) Ebel, J. P.; Anderson, J. L.; Prieve, D. C. *Langmuir* **1988**, *4*, 396.
(25) Chang, Y. C.; Keh, H. J. *J. Colloid Interface Sci.* **2008**, *322*, 634.
(26) Lou, J.; Lee, E. *J. Phys. Chem. C* **2008**, *112*, 2584.
(27) Chen, P. Y.; Keh, H. J. *J. Colloid Interface Sci.* **2005**, *286*, 774.
(28) Keh, H. J.; Hsu, L. Y. *Microfluid. Nanofluid.* **2008**, *5*, 347.
(29) Keh, H. J.; Ma, H. C. *J. Power Source* **2008**, *180*, 711.
(30) Qian, S.; Das, B.; Luo, X. *J. Colloid Interface Sci.* **2007**, *315*, 721.
(31) Rodriguez, V. V.; Busscher, H. J.; Norde, W.; van der Mei, H. C. *Electrophoresis* **2002**, *23*, 2007.
(32) Ji, J. H.; Bae, G. N.; Yun, S. H.; Jung, J. H.; Noh, H. S.; Kim, S. S. *Aerosp. Sci. Technol.* **2007**, *41*, 786.
(33) Leitch, E. C.; Willcox, M. D. P. *Curr. Eye Res.* **1999**, *19*, 12.
(34) de Kerchove, A. J.; Weroski, P.; Elimelech, M. *Langmuir* **2007**, *23*, 12301.
(35) Bos, R.; van der Mei, H. C.; Busscher, H. J. *Biophys. Chem.* **1998**, *74*, 251.
(36) Li, Y.; Lin, S. T.; Goddard, W. A. *J. Am. Chem. Soc.* **2004**, *126*, 1872.
(37) Kvarla, J. *Langmuir* **2007**, *23*, 5305.
(38) Zydney, A. L. *J. Colloid Interface Sci.* **1995**, *169*, 476.
(39) Keh, H. J.; Li, Y. L. *Langmiur* **2007**, *23*, 1061.
(40) He, Y. Y.; Lee, E. *Chem. Eng. Sci.* **2008**, *63*, 5719.
(41) O'Brien, R. W.; White, L. R. *J. Chem. Soc., Faraday Trans. 2* **1978**, *74*, 1607.
(42) Keh, H. J.; Chen, W. C. *J. Colloid Interface Sci.* **2006**, *296*, 710.
(43) Hsu, J. P.; Chen, Z. C. *J. Colloid Interface Sci.* **2007**, *314*, 256.
(44) Masliyah, J. H.; Bhattacharjee, S. *Electrokinetic Transport Phenomena*, 4th ed.; Wiley: New York, 2006.
(45) Lee, E.; Chu, J. W.; Hsu, J. P. *J. Chem. Phys.* **1999**, *110*, 11643.
(46) Lou, J.; He, Y. Y.; Lee, E. *J. Colloid Interface Sci.* **2006**, *299*, 443.
(47) Hsu, J. P.; Yeh, L. H.; Ku, M. H. *J. Colloid Interface Sci.* **2007**, *305*, 324.
(48) Hsu, J. P.; Yeh, L. H. *J. Chin. Inst. Chem. Eng.* **2006**, *37*, 601.
(49) Happel, J.; Brenner, H. *Low-Reynolds Number Hydrodynamics*; Nijhoff: Boston, MA, 1983.
(50) *FlexPDE*, version 2.22; PDE Solutions Inc.: Spokane Valley, WA, 2001.
(51) Keh, H. J.; Wei, Y. K. *Langmuir* **2000**, *16*, 5289.

JP9014417